DATA ANALYTICS AND APPLIED MATHEMATICS
E-ISSN: 2773-4854
VOLUME 5, ISSUE 2, 2024, 35 – 42
DOI: https://doi.org/10.15282/daam.v5i2.13000

RESEARCH ARTICLE

Magnetohydrodynamic flow and convective heat transfer of hybrid ferrofluid towards stagnation point on horizontal flat plate

Siti Hanani Mat Yasin[1]*, Mohd Zuki Salleh[1], Zulkhibri Ismail[1], Muhammad Khairul Anuar Mohamed[1], Dumitru Vieru[2]

[1]Centre for Mathematical Sciences, Universiti Malaysia Pahang Al-Sultan Abdullah, Lebuh Persiaran Tun Khalil Yaakob, 26300 Kuantan, Pahang, Malaysia
[2]Department of Theoretical Mechanics, Technical University of Iasi, 700050 Iasi, Romania

ABSTRACT – Ferrofluid is broadly used for dissipating heat for devices and equipment with an applied magnetic field. However, the conventional ferrofluid needs to be improved to achieve higher thermal conductivity, better heat dissipation and improved stability. Therefore, this study examines the hybrid ferrofluid flow and convective heat transfer at the stagnation point on a horizontal flat plate in the presence of a magnetic field and thermal radiation. A hybrid ferrofluid is composed of magnetite (Fe_3O_4) ferroparticles and copper (Cu) nanoparticles in water base fluid employed in this investigation. The interaction between the hybrid ferrofluid flow and the heated surface is measured using the modified boundary layer mathematical model. These equations are simplified using the similarity transformation, then solved numerically by the Keller-box method, which is implemented in MATLAB software. The influence of particle volume fraction, magnetic parameter and thermal radiation parameter on the flow field is studied. The results of the velocity profile, temperature profile and Nusselt number for the hybrid ferrofluid are compared with conventional ferrofluid to discover the hybrid ferrofluid's performance. It is found that a reduced Nusselt number rate for the hybrid ferrofluid increases compared to the conventional ferrofluid between 2.01% and 2.34%. Consequently, the hybrid ferrofluid has better thermomagnetic convection properties than conventional ferrofluid, which is probably suitable for use in various electronic devices or equipments.

ARTICLE HISTORY
Received : 20th June 2024
Revised : 20th Aug 2024
Accepted : 16th Sept 2024
Published : 30th Sept 2024

KEYWORDS
Ferrofluid
Hybrid nanofluid
Convective heat transfer
Magnetohydrodynamic
Flat plate

1. INTRODUCTION

The engineering and technical industrial constraints in heating and cooling systems are critically important, as the systems directly affect the work performance, energy efficiency, safety and product quality. Fluids are essential in the heat transfer process to carry and distribute the thermal energy efficiently. Therefore, the fluid dynamics studies are implemented to predict and understand the fluid behaviour interacting with the surroundings. Ferrofluid have recently gained extensive interest among researchers due to the properties of the fluid promising potential for use in various electronics devices or equipment, and automotive thermal management [1-2].

The composition of ferrofluid can be classified into conventional, hybrid or ternary ferrofluid. These three types differ according to the number of nanoparticles dispersed in a base fluid. Ferrofluid is composed of at least one magnetic nanoparticle suspended in a base fluid. Hence, the conventional ferrofluid contains one magnetic nanoparticle. Meanwhile, hybrid and ternary ferrofluids contain two and three different types of nanoparticles, respectively, which consist of magnetic and non-magnetic nanoparticles. Urmi et. al. [3] and Adun et al. [4] in their review paper found that the hybrid and ternary nanofluids provide better thermal transfer characteristics than conventional nanofluid.

Another study by Adogbeji et al. [5-6] in their experimental study discovered that the presence of a magnetic field on Fe_3O_4-TiO_2/water optimises the heat transfer system. Meanwhile, Taşkesen et al. [7] developed an artificial neural network based on the experimental studies of Fe_3O_4-Cu/water to obtain heat transfer performance under the magnetic field without mathematical model derivation.

Exploration into the theoretical studies of Fe_3O_4-Cu/water on a nonlinear shrinking/stretching surface by Lund et al. [8] reveals that the velocity of the hybrid ferrofluid decreases when elevating the magnetic parameter. Waqas et al. [9] continued the investigation of the hybrid ferrofluid at the stagnation point on the horizontal stretchable surface by considering the Fe_3O_4-CuO/water. The authors observed that the heat transfer rate of Fe_3O_4-CuO/water was larger than CuO/water. Next, Zainodin et al. [10] discussed the numerical solutions for Fe_3O_4-$CoFe_2O_4$/water over the nonlinearly moving surface and discovered that the heat transfer rate of the hybrid ferrofluid increases between 8.75% to 10.65% when the strength of the magnetic field grows.

The above-mentioned literature shows that the hybrid ferrofluid can enhance the heat transfer and achieve better results compared to the conventional ferrofluid. As a result, this study aims to examine the hybrid ferrofluid flow behaviour and convective heat transfer at the stagnation point on a stationary horizontal flat plate. This paper is an extension of the conventional ferrofluid flow on a horizontal flat plate study by Yasin et al. [11–14].

***CORRESPONDING AUTHOR | Siti Hanani Mat Yasin** | ✉ hananimatyasin@gmail.com
© The Author(s) 2024. Published by University Malaysia Pahang Al-Sultan Abdullah Publishing. This is an open access article under the CC BY-NC 4.0 International license.

2. MATHEMATICAL FORMULATION

The type of hybrid ferrofluid flow is determined to visualise the physical phenomena occurring on the horizontal flat plate before formulating the mathematical solutions. In this study, the fluid flow is considered two-dimensional, incompressible, steady, laminar and occurs over the external flow on the horizontal flat plate. The investigation of hybrid ferrofluid flow and convective heat transfer is focusing on the stagnation point in the presence of a magnetic field and thermal radiation, as illustrated in Figure 1. The fluid performance is discovered using the boundary layer theory by assuming the T is hybrid ferrofluid temperature and T_∞ is ambient temperature. The hybrid ferrofluid starts to flow far from the surface with the free stream velocity $U_\infty = bx$ where b is constant flow, then the fluid touches the flat plate where the surface temperature is denoted as T_w. The uniform magnetic field B_o act a transverse magnetic field whose direction is applied in the positive direction y axis with a velocity component u and always perpendicular to the horizontal flat plate along the x axis with a velocity component v.

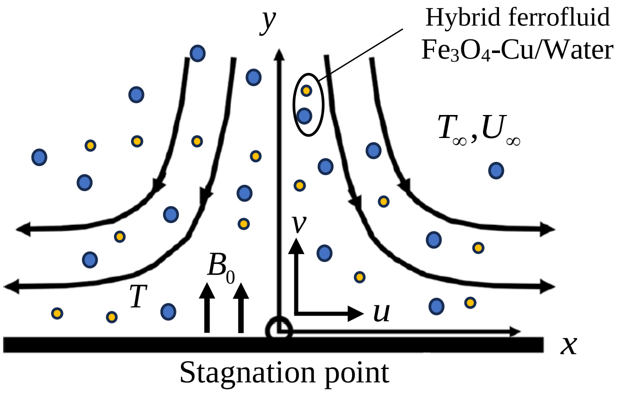

Figure 1. Physical model

Based on the assumptions stated, the governing equations are solved using the boundary layer approximation and the Boussinesq approximation produces the continuity, momentum and energy equations as below by referring to the mathematical formulation [14,15]

$$\frac{\partial u}{\partial x} + \frac{\partial v}{\partial y} = 0, \tag{1}$$

$$u\frac{\partial u}{\partial x} + v\frac{\partial u}{\partial y} = U_\infty \frac{\partial U_\infty}{\partial \overline{x}} + v_{hff}\frac{\partial^2 u}{\partial y^2} + \frac{\sigma_{hff}\left(B_o^2\right)}{\rho_{hff}}\left(U_\infty - u\right), \tag{2}$$

$$u\frac{\partial T}{\partial x} + v\frac{\partial T}{\partial y} = \alpha_{hff}\frac{\partial^2 T}{\partial y^2} + \frac{1}{\left(\rho C_p\right)_{hff}}\frac{16\sigma^* T_\infty^3}{3k^*}\frac{\partial^2 T}{\partial y^2}, \tag{3}$$

subject to the Blasius flow, no-slip velocity and constant wall temperature condition

$$\begin{gathered} u = 0,\ v = 0,\ T = T_w \ \text{ at } y = 0, \\ u \to 0,\ T \to T_\infty \ \text{ at } y \to \infty. \end{gathered} \tag{4}$$

where subscript *hff* is hybrid ferrofluid, $v_{hff}, \sigma_{hff}, \rho_{hff}, \alpha_{hff}, \left(\rho C_p\right)_{hff}$ is the thermophysical properties that can be defined as presented in Table 1, which are expressed in terms of nanoparticles (subscript *s*), conventional ferrofluid (subscript *ff*), base fluid (subscript *f*) and particle volume fraction ϕ. Meanwhile, $\frac{16\sigma^* T_\infty^3}{3k^*}\frac{\partial^2 T}{\partial y^2}$ is a simplified expression of the radiative heat flux, which can be solved using the Rosseland approximation and Taylor series, as shown in [14] with σ^* and k^* is the Stefan-Boltzmann constant and the mean absorption, respectively.

Table 1. The theoretical model for the thermophysical properties of hybrid ferrofluid [10,15]

Physical properties	Equations
Density	$\rho_{hff}=\left(1-\phi_2\right)\left[\left(1-\phi_1\right)\rho_f+\phi_1\rho_{s1}\right]+\phi_2\rho_{s2}$
Electrical conductivity	$\sigma_{hff}=\left[\dfrac{\sigma_{s2}+2\sigma_{ff}-2\phi_2\left(\sigma_{ff}-\sigma_{s2}\right)}{\sigma_{s2}+2\sigma_{ff}+\phi_2\left(\sigma_{ff}-\sigma_{s2}\right)}\right]\sigma_{ff}$ where $\sigma_{ff}=\left[\dfrac{\sigma_{s1}+2\sigma_f-2\phi_1\left(\sigma_f-\sigma_{s1}\right)}{\sigma_{s1}+2\sigma_f+\phi_1\left(\sigma_f-\sigma_{s1}\right)}\right]\sigma_f$
Dynamic viscosity	$\mu_{hff}=\dfrac{\mu_f}{\left(1-\phi_1\right)^{2.5}\left(1-\phi_2\right)^{2.5}}$
Kinematic viscosity	$v_{hff}=\dfrac{\mu_{hff}}{\rho_{hff}}$
Thermal diffusivity	$\alpha_{hff}=\dfrac{k_{hff}}{\left(\rho C_p\right)_{hff}}$
Specific heat capacity	$\left(\rho C_p\right)_{hff}=\left(1-\phi_2\right)\left[\left(1-\phi_1\right)\left(\rho C_p\right)_f+\phi_1\left(\rho C_p\right)_{s1}\right]+\phi_2\left(\rho C_p\right)_{s2}$
Thermal conductivity	$k_{hff}=\left[\dfrac{k_{s2}+2k_{ff}-2\phi_2\left(k_{ff}-k_{s2}\right)}{k_{s2}+2k_{ff}+\phi_2\left(k_{ff}-k_{s2}\right)}\right]k_{ff}$ where $k_{ff}=\dfrac{k_{s1}+2k_f-2\phi_1\left(k_f-k_{s1}\right)}{k_{s1}+2k_f+\phi_1\left(k_f-k_{s1}\right)}k_f$

Besides, the subscripts *1* and *2* symbolise the different types of nanoparticles, where *1* represents the magnetite (Fe_3O_4) ferroparticles, while *2* is the copper (Cu) nanoparticles. It is crucial to mention here that the thermophysical properties have a specific value that must be used during the implementation of numerical analysis, as demonstrated in Table 2.

Table 2. The value of thermophysical properties [15–17]

Physical Properties	Water	Fe_3O_4	Cu
Density, $\rho\left(kg/m^3\right)$	997.1	5200	8933
Specific heat capacity, $C_p\left(J/kgK\right)$	4179	670	385
Thermal conductivity, $k\left(W/mK\right)$	0.613	6	400
Electrical conductivity, $\sigma\left(s/m\right)$	0.05	25000	59600000

Next, the adequate similarity transformation is carried out on the nonlinear partial differential equations (1) –(3) and equation (4) in terms of η using the variables:

$$\eta=\left(\frac{b}{v_f}\right)^{1/2}y,\quad \psi=\left(bv_f\right)^{1/2}xf(\eta),\quad \theta(\eta)=\frac{T-T_\infty}{T_w-T_\infty}, \tag{5}$$

where $f\left(\eta\right)$ is the dependent variable, b is a positive constant and the stream function ψ can be defined as

$$u=\frac{\partial\psi}{\partial y},v=-\frac{\partial\psi}{\partial x}, \tag{6}$$

gives the following equations

$$u=bxf'\left(\eta\right),v=-\left(bv_f\right)^{1/2}f\left(\eta\right), \tag{7}$$

which satisfied equation (1) and obtained the nonlinear dimensionless ordinary differential equations as follows

$$\frac{1}{(1-\phi_1)^{2.5}(1-\phi_2)^{2.5}\left(\rho_{hff}/\rho_f\right)}f'''+ff''-f'^2+1+\frac{\left(\sigma_{hff}/\sigma_f\right)}{\left(\rho_{hff}/\rho_f\right)}M\left(1-f'\right)=0, \tag{8}$$

$$\frac{1}{\Pr}\left(\frac{(\rho C_p)_f}{(\rho C_p)_{hff}}\right)\left(\frac{k_{hff}}{k_f}+\frac{4}{3}Nr\right)\theta''+f\theta'=0, \tag{9}$$

with the boundary conditions

$$\begin{gathered} f(0)=0, f'(0)=0, \theta(0)=1, \\ f'(\eta)\rightarrow 1, \theta(\eta)\rightarrow 0 \quad \text{as} \quad y\rightarrow\infty, \end{gathered} \tag{10}$$

where the primes describe the differentiation respect to η, the magnetic parameter *M*, the Prandtl number Pr and the thermal radiation *Nr* defined as

$$M=\frac{\sigma_f B_o^{\,2}}{\rho_f b}, \ \Pr=\frac{\nu_f\left(\rho C_p\right)_f}{k_f} \ \text{and} \ Nr=\frac{4\sigma^* T_\infty^3}{k^* k_f}. \tag{11}$$

Then, the skin friction coefficient $C_f=\dfrac{\tau_w}{\rho_f U_\infty^2}$ where $\tau_w=\mu_{hff}\left(\dfrac{\partial u}{\partial y}\right)_{y=0}$ and the local Nusselt number $Nu_x=\dfrac{xq_w}{k_f\left(T_w-T_\infty\right)}$ where $q_w=-k_{hff}\left(\dfrac{\partial T}{\partial \bar{y}}\right)_{\bar{y}=0}+q_r$ and $q_r=-\dfrac{4\sigma^*}{3k^*}\left(\dfrac{\partial T^4}{\partial \bar{y}}\right)$ is written in the dimensionless form using the similarity transformation method, yields the reduced skin friction coefficient and reduced Nusselt number, respectively, as follows

$$C_f \operatorname{Re}_x^{1/2}=\frac{f''(0)}{(1-\phi_1)^{2.5}(1-\phi_2)^{2.5}} \ \text{and} \ Nu_x \operatorname{Re}_x^{-1/2}=-\left(\frac{k_{hff}}{k_f}+\frac{4}{3}Nr\right)\left(\theta'(0)\right), \tag{12}$$

where $\operatorname{Re}_x=\dfrac{U_\infty x}{\nu_f}$ the local Reynolds number.

3. RESULTS AND DISCUSSION

The nonlinear dimensionless ordinary differential equations (8) and (9) with boundary conditions (10) were solved numerically using the Keller-Box method. Then, the numerical algorithm was run in MATLAB software with the boundary layer thickness $\eta_\infty=3$ and the step size $\Delta\eta=0.01$. The effect of particle volume fraction ϕ, the magnetic parameter *M* and thermal radiation *Nr* of the hybrid ferrofluid and the conventional ferrofluid at the stagnation point on a horizontal flat plate towards the velocity profile $f'(\eta)$, temperature profile $\theta(\eta)$, reduced skin friction coefficient $C_f \operatorname{Re}_x^{1/2}$ and reduced Nusselt number $Nu_x \operatorname{Re}_x^{-1/2}$ will be discussed. The numerical results of $f'(\eta)$ and $\theta(\eta)$ are illustrated graphically, while the results of $C_f \operatorname{Re}_x^{1/2}$ and $Nu_x \operatorname{Re}_x^{-1/2}$ are presented in tabular form with Pr = 6.2 (water). The comparison between the present outcomes and the previous study has been made to verify the derivation and program codes. Table 3 shows that the current results are in significant agreement with Khan et al. [18] and Yasin et al. [14], hence verify the precision of the current output. Noteworthy to mention, the comparison displayed is the hybrid ferrofluid reduced to the regular fluid with the absence of ϕ, *M* and *Nr,* as well as the value of Pr = 3, 6 and 10, to make the current output comparable with the previous results. Meanwhile, the parameter value of ϕ, *M* and *Nr* are followed from the previous study by Taşkesen et al. [7] and Zainodin et al. [10].

Table 3. Comparison values of $-\theta'(\eta)$ when $\phi=M=Nr=0$ for variation of Pr

Pr	Khan et al. [18]	Yasin et al. [14]	Present
3	0.8652	0.8652	0.8652
6	1.1147	1.1147	1.1147
10	1.3388	1.3389	1.3389

Table 4. Variations of $Nu_x \operatorname{Re}_x^{-1/2}$ for conventional ferrofluid and hybrid ferrofluid

	Conventional ferrofluid ($\phi_1=0.01, \phi_2=0$)				Hybrid ferrofluid ($\phi_1=\phi_2=0.01$)			
Nr	M = 0	M =1	M = 2	M = 5	M = 0	M =1	M = 2	M = 5
0	1.1461	1.2147	1.2623	1.3518	1.1751	1.2422	1.2895	1.3786
1	1.9445	2.0469	2.1171	2.2468	1.9712	2.0703	2.1390	2.2669

Figures 2 and 3 depict the effect of particle volume fraction ϕ on the velocity profile and temperature profile for both ferrofluids. It can be seen that an increment of ϕ, the velocity profile for both ferrofluids increases as shown in Figure 2. Besides, the velocity profile of the hybrid ferrofluid is higher than the conventional ferrofluid. Generally, the viscosity of the hybrid ferrofluid is escalating compared to the conventional ferrofluid because of additional nanoparticles. As a result, the velocity profile of the hybrid ferrofluid should be lower than the conventional ferrofluid. But, contrary phenomena occur due to the thermal conductivity of Cu being higher than Fe_3O_4, which significantly enhances the heat dissipation. This allows heat to spread faster, then causes low viscosity of the hybrid ferrofluid to absorb more heat and move farther from the heated surface, especially with the presence of thermal radiation. Consequently, the temperature rises more gradually and leading to a thicker thermal boundary layer as portrayed in Figure 3.

Apart from that, the effect of magnetic parameter *M* plotted in Figures 4 and 5 is essential to discover because of Fe_3O_4 is very responsive to the magnetic field, which enables better thermomagnetic convection. Figures 4 and 5 reveal that the hybrid ferrofluid has a higher velocity than conventional ferrofluid, even though the temperature decreases and the thermal boundary layer thickens with increasing magnetic field under thermal radiation. This phenomenon is different when augmenting the particle volume fraction, although the magnetic field exists. Theoretically, the magnetic field induces the Lorentz force that drives fluid motion more efficiently and decreases the temperature. This factor could not reduce the hybrid ferrofluid velocity, particularly if the momentum boundary layer stays thin as shown in Figure 4 because of Cu maintain lower viscosity, lower resistance and better heat transport under magnetic force.

Table 4 demonstrates the effect of various parameters on the reduced Nusselt number. It is vital to mention here that the skin friction coefficient is not displayed in the numerical results because unique values exist when amending the thermal radiation parameter caused by the decoupling of boundary layer equations. When *M* and *Nr* upsurge, the Nusselt number of the hybrid ferrofluid is observed to be higher than the conventional ferrofluid. As stated above, the hybrid ferrofluid has a higher thermal conductivity, lower viscosity and higher heat absorption under the magnetic field and thermal radiation due to Cu, which provides a stronger thermomagnetic convection. From this outcome, when the Nusselt number is high, it produces stronger convection and makes the hybrid ferrofluid more effective for heat transfer.

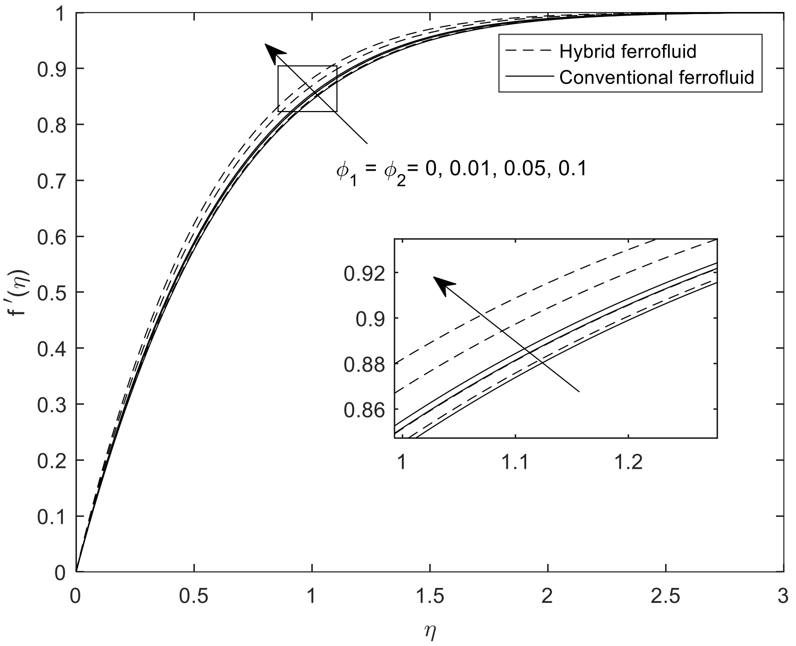

Figure 2. Effect of various ϕ_1 and ϕ_2 on $f'(\eta)$ when *M = 1* and *Nr = 1*

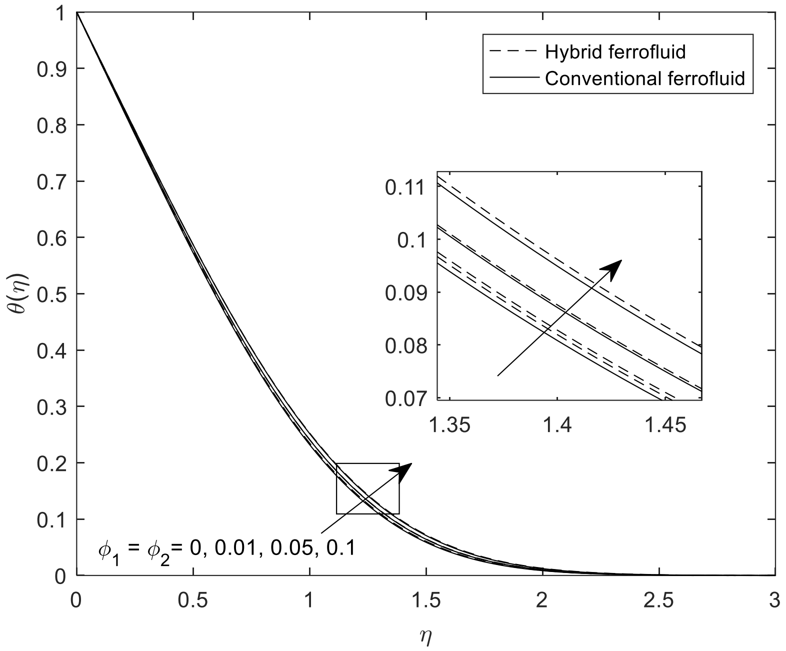

Figure 3. Effect of various ϕ_1 and ϕ_2 on $\theta(\eta)$ when *M = 1* and *Nr = 1*

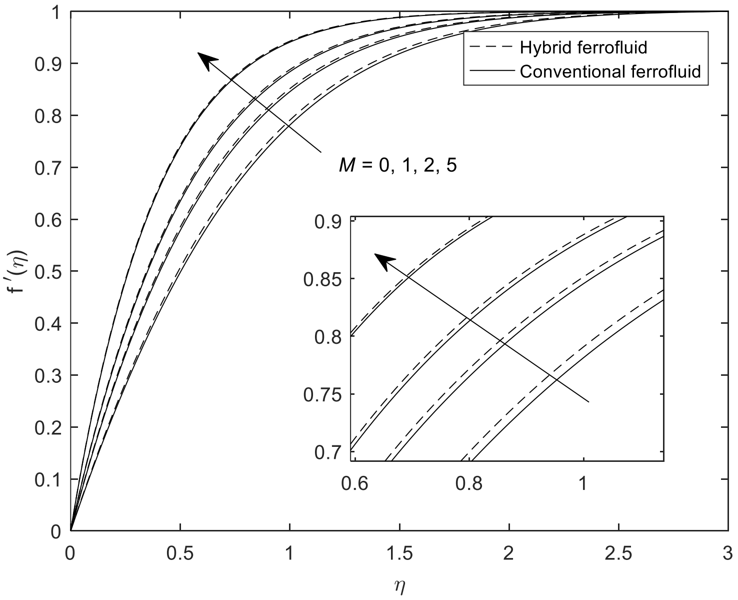

Figure 4. Effect of various *M* on $f'(\eta)$ when $\phi_1 = \phi_2 = 0.01$ and *Nr = 1*

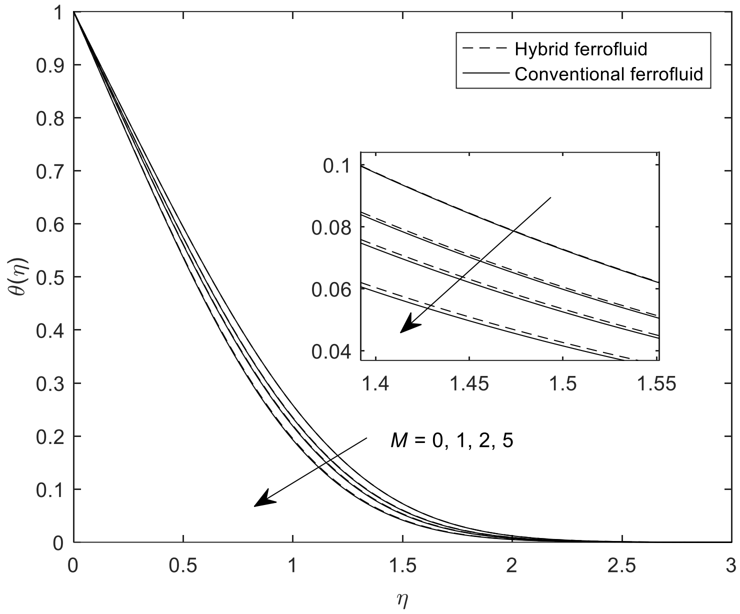

Figure 5. Effect of various M on $\theta(\eta)$ when $\phi_1 = \phi_2 = 0.01$ and $Nr = 1$

4. CONCLUSIONS

This study has explored the efficiency of Fe_3O_4-Cu/water hybrid ferrofluid, which extends from Fe_3O_4/water conventional ferrofluid with a focus on magnetohydrodynamic flow and convective heat transfer performance. The critical discoveries found the vital role of Cu nanoparticles added to conventional ferrofluid in order to improve the fluid flow and enhance the convective heat transfer. In conclusion, Fe_3O_4-Cu/water hybrid ferrofluid has a stronger thermomagnetic convection compared to Fe_3O_4/water conventional ferrofluid. For future studies, to address the issue of unique value arising from decoupling boundary conditions, it is possible to replace the linear thermal radiation terms with nonlinear thermal radiation terms. Besides, an in-depth investigation of ferrofluid flow and convective heat transfer could be conducted using ternary ferrofluids to enhance high-efficiency cooling performance.

ACKNOWLEDGEMENTS

Institution(s)
All authors would like to express their gratitude to Universiti Malaysia Pahang Al-Sultan Abdullah Technical University of Iasi for the support and facilities.

Fund
The authors would like to thank the Ministry of Higher Education for providing financial support under Fundamental Research Grant Scheme (FRGS) No. FRGS/1/2024/STG06/UMP/02/9 (University reference RDU240132).

Individual Assistant
NA

AUTHOR CONTRIBUTIONS

Siti Hanani Mat Yasin (Conceptualisation; Methodology, Resources; Writing- original draft), Mohd Zuki Salleh (Conceptualisation; Writing- review & editing), Zulhibri Ismail (Methodology; Writing- review & editing), Muhammad Khairul Anuar Mohamed (Resources; Writing- review & editing), Dumitru Veiru (Writing- review & editing).

DECLARATION OF ORIGINALITY

The authors declare no conflict of interest to report regarding this study conducted.

REFERENCES

[1] Oehlsen O, Cervantes-Ramírez SI, Cervantes-Avilés P, Medina-Velo IA. Approaches on ferrofluid synthesis and applications: Current status and future Perspectives. ACS Omega. 2022; 7:3134-3150.
[2] Hwang SG, Garud KS, Seo JH, Lee MY. Heat flow characteristics of ferrofluid in magnetic field patterns for electric vehicle power electronics cooling. Symmetry. 2022; 14: 1-13.
[3] Urmi WT, Shafiqah AS, Rahman MM, Kadirgama K, Maleque MA. Preparation methods and challenges of hybrid

nanofluids: A review. Journal of Advanced Research in Fluid Mechanics and Thermal Sciences. 2021; 78: 56-66.
[4] Adun H, Kavaz D, Dagbasi M. Review of ternary hybrid nanofluid: Synthesis, stability, thermophysical properties, heat transfer applications, and environmental effects. Journal of Cleaner Production. 2021; 328.
[5] Adogbeji VO, Govinder K, Sharifpur M, Meyer JP. Experimental investigation of the effect of magnetic field placement on pressure drop, entropy generation, heat transfer, and thermal performance of Fe_3O_4/TiO_2 magnetic nanofluids in turbulent flow. Powder Technology. 2025; 466: 1-24.
[6] Adogbeji VO, Sharifpur M, Meyer JP. Experimental investigation of heat transfer enhancement, thermal efficiency, and pressure drop in forced convection of magnetic hybrid nanofluid (Fe_3O_4/TiO_2) under varied magnetic field strengths and waveforms. Case Study in Thermal Engineering. 2024; 63: 1-23.
[7] Taşkesen E, Dirik M, Tekir M, Pazarlioğlu HK. Predicting heat transfer performance of Fe_3O_4-Cu/water hybrid nanofluid under constant magnetic field using ANN. Journal of Thermal Engineering. 2023; 9: 811-822.
[8] Lund LA, Omar Z, Raza J, Khan I. Magnetohydrodynamic flow of Cu–Fe_3O_4/H_2O hybrid nanofluid with effect of viscous dissipation: Dual similarity solutions. Journal of Thermal Analysis Calorimetry. 2021: 143: 915-927.
[9] Waqas H, Khan SA, Muhammad T, Naqvi SMRS. Heat transfer enhancement in stagnation point flow of ferro-copper oxide/water hybrid nanofluid: A special case study. Case Study in Thermal Engineering. 2021; 28: 1-13.
[10] Zainodin S, Jamaludin A, Nazar R, Pop I. MHD mixed convection flow of hybrid ferrofluid through stagnation-point over the nonlinearly moving surface with convective boundary condition, viscous dissipation, and joule heating effects. Symmetry. 2023; 15: 1-29.
[11] Yasin SHM, Mohamed MKA, Ismail Z, Widodo B, Salleh MZ, Numerical solution on MHD Stagnation point flow in ferrofluid with Newtonian heating and thermal radiation effect. CFD Lettters. 2019; 11: 21–31.
[12] Yasin SHM, Mohamed MKA, Ismail Z, Widodo B, Salleh MZ. MHD flow and heat transfer of ferrofluid on stagnation point along flat plate with convective boundary condition and thermal radiation effect. Journal of Physics: Conference Series. 2019. 1366: 1–9.
[13] Yasin SHM, Mohamed MKA, Ismail Z, Salleh MZ. MHD free convection boundary layer flow near the lower stagnation point flow of a horizontal circular cylinder in ferrofluid. IOP Conference Series: Materials Science and Engineering. 2020; 736: 1-12.
[14] Yasin SHM. Magnetohydrodynamic flow and heat transfer of ferrofluid over a flat plate, circular cylinder and sphere. PhD Thesis. Universiti Malaysia Pahang Al-Sultan Abdullah, 2025.
[15] You X, Wang Y. Series solutions of three-dimensional magnetohydrodynamic hybrid nanofluid flow and heat transfer. Nanomaterials. 2024; 14: 1-19.
[16] Zitouni K, Boumaaza M, Aidaoui L et al.. Numerical assessment of heat transfer and entropy generation of a mixed convection ferrofluid flow under the effect of a non-uniform magnetic field. Case Study in Thermal Engineering. 2025; 66: 1-30.
[17] Hasan MM, Uddin MJ, Faroughi SA. Magnetohydrodynamic nanofluids flow and heat transfer with radiative heat flux and exothermic chemical reactions. International Journal of Thermofluids. 2025; 26: 1-19.
[18] Khan WA, Culham R, Haq RU. Heat transfer analysis of MHD water functionalized carbon nanotube flow over a static/moving wedge. Journal of Nanomaterials. 2015; 2015: 1-13.